5-2015

Population Dynamics in Active Galactic Nuclei

Jon Bessler
University of Arkansas, Fayetteville

Population Dynamics in Active Galactic Nuclei

Population Dynamics in Active Galactic Nuclei

A thesis submitted in partial fulfillment
of the requirements for the degree of
Master of Science in Physics

by

Jon Bessler
University of Arkansas
Bachelor of Science in Physics, 2013

May 2015
University of Arkansas

This thesis is approved for recommendation to the Graduate Council.

_____
Dr. Julia Kennefick
Thesis Director

_____
Dr. Daniel Kennefick
Committee Member

_____
Dr. William Oliver
Committee Member

_____
Dr. Mark Arnold
Committee Member

Abstract

The goal of this thesis is to present an approach to understanding the dynamics that govern the evolution of active galactic nuclei (AGN) in general, and those associated with spiral galaxies in particular. This approach starts with the continuity equation governing the mass function for a population of supermassive black holes (SMBHs). This approach is then extended to the luminosity function for AGN. Where the dynamical parameters that govern accretion are fairly well known, those values are adopted. The values that are not as well known are constrained by comparing evolved luminosity functions with observed luminosity functions. Boundary conditions for this model are typically taken to be locally observed mass functions unless otherwise specified.

It can be concluded that the Eddington ratio is likely a function of time and possibly a function of mass. The duty cycle is likely a function of both time and mass. The qualitative evolution of the Eddington ratio and duty cycle can be inferred from the luminosity evolution and density evolution of observed luminosity functions respectively. Additionally, models with a break in the duty cycle agree well with observations. This may be an indication of feedback within the host galaxy. The effect of mergers is also examined briefly, and the results imply lower Eddington ratios than models without mergers.

Acknowledgements

I would like to thank my advisers, Dr. Julia Kennefick and Dr. Daniel Kennefick, for their support throughout this project. It was their encouragement that allowed me to pursue this idea to fruition. Had I not had their expertise and oversight, I would not have been able to accomplish this.

I would also like to thank my wife, Lori, for her support. She has been extremely tolerant of my research. Her advice, though not related directly to my research, was invaluable. I could not have been able to see this project through had it not been for her encouragement.

I thank my children, Tobias and Layla, for their patience and understanding as I have worked on this project.

I also would like to thank my parents, Jack and Janet, and my grandmother Kathryn. Without their support, my academic endeavors would not have been possible.

Contents

List of Figures

1 Introduction

The class of objects broadly described as active galactic nuclei (AGN) are among the most luminous objects observed in the visible universe. There has been much interest in understanding their evolution on cosmological time scales. Since it has been shown that there are correlations between AGN and their host galaxies [6, 7, 8], it is hoped that understanding AGN evolution will give insights into galaxy evolution.

The most distant and luminous of the AGN are quasars. The original observations of quasars led to the belief that they were stellar in nature and reside within our galaxy. It was only when Schmidt [16] recognized their high redshift, that they were understood to be extragalactic in nature, and much more distant than any previously observed galactic nucleus. In order to account for the extreme distances at which quasars are visible, it is necessary to develop some mechanism which can produce the extreme luminosities observed. Salpeter [15] noted that the source of energy for these AGN could be material falling into the supermassive black hole (SMBH) that resides at the center of the galaxy associated with the AGN.

Following this, there has been much interest in uncovering the details of accretion. To understand more about these objects, many surveys have been carried out to catalog AGN and their associated properties. With sufficiently large surveys, one can obtain a luminosity function which describes the number density of quasars as a function of their luminosity [17].

Applying a conservation equation to these luminosity functions can yield insights into their evolution. The results of these models are then compared with the observed luminosity and mass functions in order to constrain the parameters that govern accretion. This is a

continuation of work done by Cavaliere et al. [3, 4], Small and Blandford [23], and Shankar et al. [18, 19].

The continuity equation itself will be discussed in Chapter 2. The implementation of this and some discussion of the parameters of accretion will be considered in Chapter 3. The actual models developed for this research will be discussed in Chapter 4. In Chapter 5, an alternative approach to modeling AGN evolution will be discussed. The results will be summarized in Chapter 6.

2 The Continuity Equation

One approach that has been employed to develop models of AGN evolution is to apply the continuity equation to mass and luminosity functions. The general approach is to take an observed mass or luminosity function at a particular redshift and extrapolate that function to other redshifts, assuming a particular cosmic evolution. The evolved functions can then be compared to observations in order to constrain the details of accretion.

2.1 Mass Function

The starting point for developing these models is to use the analysis of Small and Blandford [23]. A mass function, $N(M,t)$, of supermassive black holes must obey the following continuity equation:

$$\frac{\partial N}{\partial t} + \frac{\partial}{\partial M}(N\langle \dot{M} \rangle) = S(M,t) \tag{2.1}$$

where N is the number density of supermassive black holes and M is the mass of the black hole.

$S(M,t)$ is a source function that describes the introduction or removal of black holes from the system, either through creation or mergers. The bulk of the observations made with respect to AGN are out to redshift $z \approx 6$. It will therefore be assumed that the dynamics relating to AGN evolution developed in these models are valid only in this regime $(0 < z < 6)$. It will be also be assumed going forward that the source function does not contribute to the growth in number of black holes; the bulk of the black holes were formed before redshift $z \approx 6$. The source term will then only account for mergers.

The most straightforward way to infer accretion rates for an active galactic nucleus would be to consider the luminosity. By assuming that there is a conversion of in-falling matter into radiative energy, the relation is as follows

$$L = \epsilon \dot{M} c^2 \tag{2.2}$$

where L is the luminosity and ϵ is an efficiency parameter that governs how much in-falling matter is converted into radiative energy. Now accretion rates are limited, on average, by the radiation pressure. This leads to a limiting luminosity, the Eddington limit,

$$L_E = \frac{4\pi G M m_p c}{\sigma_T}$$

where m_p is the proton mass and σ_T is the Thomson scattering cross-section [14]. Expressing the ratio of the luminosity to the Eddington limit as $\lambda = L/L_E$ gives an average accretion rate that is

$$\langle \dot{M} \rangle = \frac{\lambda(1-\epsilon)}{\epsilon t_E} M \tag{2.3}$$

where the Eddington time, $t_E = \sigma_T c / 4\pi G m_p$, and the factor of $1-\epsilon$ accounts for the amount actually accreted onto the black hole.

Equation 2.3 gives the accretion rate assuming that it is a steady process. In general it is not, as evidenced by the variability in the luminosity of individual AGN. The introduction of a duty cycle parameter, δ, can account for intermittent accretion [23]. The duty cycle can be thought of as the probability of accretion for a particular black hole at a particular time.

Taking an ensemble approach, it could be defined as:

$$\delta(M,t) \equiv \frac{\Phi(L,t)_{L=M\lambda c^2/t_E}}{N(M,t)} \tag{2.4}$$

where Φ is the luminosity function. The average accretion rate then becomes

$$\langle \dot{M} \rangle = \frac{\delta\lambda(1-\epsilon)}{\epsilon t_E} M, \tag{2.5}$$

where δ, λ, and ϵ may be functions of mass, time, or both.[1] The continuity equation then becomes

$$\frac{\partial N}{\partial t} + \left[\frac{\delta\lambda(1-\epsilon)}{\epsilon t_E} M\right] \frac{\partial N}{\partial M} = S(M,t). \tag{2.6}$$

It would be much more useful to put 2.6 in a form that depends explicitly on redshift, z, and $\log M/M_\odot$. For a ΛCDM cosmology with $\Omega_m = 0.3089$ and $\Omega_\Lambda = 0.6911$ [1], the redshift-time relation can be approximated as:

$$t \approx H_0^{-1}(1+z)^{-3/2}, \tag{2.7}$$

where $H_0 = 67.74$ km s^{-1} Mpc^{-1}. This form is chosen for simplification of the PDE that follows. A comparison of this approximation and the exact closed-form relation is shown in the appendix (Fig. 7.1). So the continuity equation in terms of z and $\log M/M_\odot$ is

$$-\frac{2H_0}{3}(1+z)^{5/2}\frac{\partial N}{\partial z} + \frac{\delta\lambda(1-\epsilon)}{\epsilon t_E \ln 10}\frac{\partial N}{\partial \log M/M_\odot} = S(M,z). \tag{2.8}$$

[1] These parameters will be discussed in greater detail in Chapter 3

In principle, once parameters of accretion are found, solutions to Eq. 2.8 will give the mass evolution for a population of black holes.

2.2 Luminosity Function

Here we consider two approaches to developing a time-dependent luminosity function. The first approach is to derive a continuity equation from 2.6 and solve this. The second approach is to use the relationship between the mass function and the luminosity function and the duty cycle. These two approaches are discussed below.

2.2.1 Partial Differential Equation

The first approach begins with Eq. 2.6

$$\frac{\partial N}{\partial t} + \left(\frac{\delta \lambda (1-\epsilon)}{\epsilon t_E} M \right) \frac{\partial N}{\partial M} = S(M,t)$$

using Eqs. 2.4, 2.2, and 2.3 this can be rewritten as

$$\frac{1}{\delta} \frac{\partial \Phi}{\partial t} + \frac{\lambda (1-\epsilon)}{\epsilon t_E} L \frac{\partial \Phi}{\partial L} = \left[S(M,t) \right]_{M = L t_E / \lambda c^2} .$$

Taking this and putting it in terms of z and $\log L/L_\odot$ gives:

$$-\frac{2H_0}{3\delta}(z+1)^{5/2} \frac{\partial \Phi}{\partial z} + \frac{\lambda (1-\epsilon)}{\epsilon t_E \ln 10} \frac{\partial \Phi}{\partial \log L/L_\odot} = \left[S(M,t) \right]_{M = L t_E / \lambda c^2} . \tag{2.9}$$

Assuming appropriate boundary conditions and parameters of accretion, the luminosity function can be found directly from Eq. 2.9, without the requirement of a known mass function.

2.2.2 Duty Cycle

The second approach starts with Eq. 2.4. I have defined the duty cycle as the fraction of time a black hole is accreting (luminous) at a given time. It could, alternatively, be thought of as the fraction of black holes in a given population at a given time that are accreting on average. In both of these cases, the time which is under consideration is long compared to the fluctuations in accretion, but short compared to time scales of the universe. In this view the luminosity function can be found from

$$\Phi(L,t)_{L=M\lambda c^2/t_E} = \delta(M,t)N(M,t). \tag{2.10}$$

Solutions acquired by this method depend directly on the mass function, however they do not require an input luminosity function.

2.3 Analytical Solutions

Having set up the partial differential equations that describe the population evolution, it seems natural at this point to discuss solutions. An analytical solution may be obtained if certain simplifying assumptions are made. It is possible to assume a form for the mass or luminosity as a function of time as is done by Cavaliere et al. [3] and extract a solution. There and in [4] detailed discussion of the characteristics of various analytical solutions are presented.

While a closed-form analytical solution is desirable, it is difficult to obtain one if the parameters of accretion are functions of mass, time, or both. Additionally, the source term

may be a function of mass or time. With the introduction of these complications, a general analytical solution is extremely unlikely. The goal of this research then is to obtain numerical solutions to Eq. 2.6. The obtained solutions will take the form of interpolating functions.

3 Implementation

The parameters that govern accretion are given in Eq. 2.5. The following sections discuss these parameters in detail, specifically the forms that are adopted for an initial model. The results of this initial model are discussed. Models that incorporate refinements to the parameters will be developed and discussed in subsequent chapters.

3.1 Accretion Parameters

3.1.1 Eddington Ratio

The Eddington ratio, λ, is the parameter that links the mass of the supermassive black hole with the luminosity of the associated AGN. The value of this parameter depends upon accretion disk structure. While it is possible for supermassive black holes to accrete at super-Eddington rates, sustained accretion in this regime is not likely. Additionally, super-Eddington accretion can be considered a possible outcome for non-isotropic (accretion-disk) models. Various estimates have been given for the Eddington ratio, and it may well be a function of mass, time, or both. Work done by Kollmeier et al. [11] has shown a scattering of values with a peak of $\lambda = 0.25$ among black holes at redshifts $0.3 < z < 4$. Shankar et al. [18] (hereafter SWM09) use a value of 0.4 for their analysis.

3.1.2 Efficiency Parameter

The efficiency parameter, ϵ, depends upon the actual mechanism of mass to energy transfer. While it is possible to develop models that evolve the SMBH mass function through cosmic time without understanding the exact details of accretion, it still requires that a value be

adopted for this parameter. Using a very simplified non-relativistic calculation Peterson [14] shows that this parameter can be expected to be around $\epsilon \sim 0.1$. This estimate is based on the assumption that accreting matter falls to within 5 Schwarzschild radii. In the relativistic case the upper limit is $\epsilon \leq 0.42$ [9]. Shapiro [20] claims $\epsilon \approx 0.2$ based on magnetohydrodynamic (MHD) simulations. The value adopted in SWM09 is $\epsilon = 0.065$. For most of the models developed here I have adopted a value of 0.1.

3.1.3 Duty Cycle

The duty cycle is probably the least well understood of these parameters. It is most likely a function of both mass and time. It is possible to directly obtain an expression for the duty cycle from the mass and luminosity functions via Eq. 2.4, assuming a mass and luminosity function are available at a particular redshift. This is rather straightforward to do, however it presents difficulties as the observed luminosity functions are incomplete due to flux limits and the resulting duty cycle is only valid within a particular set of values.

While this can be used to obtain an expression for the duty cycle as a function of mass, the time dependence is not so clear. This may be found by looking at luminosity functions and mass functions to see what sort of properties the time dependence might have.

In a simplified model, the duty cycle could be considered to have exponential decay with time. It seems reasonable that an accreting body will accrete maximally when fuel is plentiful, then the accretion rate would fall off exponentially with time as fuel is used up. The mass dependence of the duty cycle could also be modeled as an exponential decay with mass since the larger mass black holes would use up their fuel first. For the first model, I

will assume a duty cycle of the form

$$\delta(M,t) = \delta_0 e^{-t/\tau} \left(\frac{M}{M_\odot}\right)^{-\mu} \tag{3.1}$$

where the terms will be discussed as follows.

The coefficient of accretion, δ_0, is the scale factor for the duty cycle given in Eq. 3.1. It is constrained to $0 < \delta_0 < 1$ by definition, and will be further constrained by fitting the evolved luminosity functions to observations.

The characteristic time, τ, gives the time scale upon which accretion, and the cessation thereof is determined. It may be a function of feedback mechanisms within the host galaxy.

The mass parameter, μ, is likely determined by the availability of fuel. In principle there are no constraints on this parameter. Values of $\mu > 1$ however, render evolution static and are highly unlikely.

3.2 Boundary Conditions

The PDE shown in Eq. 2.8 requires two boundary conditions to obtain a solution. One boundary condition is the mass function at a given redshift. For much of this research I will take a local mass function, $N(M, z \approx 0)$, and evolve it back in time to get the mass function at higher redshifts.

The other boundary condition I have imposed is that $N(\log M/M_\odot = 30, z) = 0$ since it could be safely assumed that there are no black holes in that regime. I have adopted the

initial mass function from SWM09 at $z = 0.02$:

$$N(M, 0.02) = \frac{10^{-2.969}}{\left(\frac{M}{10^{8.689} M_\odot}\right)^{0.4320} + \left(\frac{M}{10^{8.689} M_\odot}\right)^{1.871}} \tag{3.2}$$

This is a best-fit double power law from the tabulated data presented in SWM09.

3.3 Mergers

The data presented in the appendix, from models using the continuity equation, ignore the effect of mergers. For all of these models, the source term $S(M, t) = 0$. The introduction of a simple source term $S < 0$ that does account for mergers causes the population as a whole to move to lower number densities. While mathematically consistent with the continuity equation, this can have the effect of introducing discontinuities or negative populations. It would seem that any representation of mergers should propagate the mass function not just to lower density, but also to higher mass. A model incorporating mergers will be discussed later in Chapter 5.

4 Models

In order to constrain the values for the parameters of accretion, numerical solutions to the continuity equation are found over the interval $0 < z < 6$ using an initial set of parameters. The results for the luminosity function were compared to those found by Hopkins et al. (hereafter HRH07) [10]. The parameters were then adjusted to get the greatest apparent match to the observed luminosity functions. The dynamics are then applied to the mass function found by Davis et al. [5] to get the evolution of the spiral galaxy BHMF and spiral AGN luminosity function.

A summary of the properties of the models that were developed can be found in Tables 7.1 and 7.2. The models are numbered, and listed in the table, in the order in which they were developed. The parameters constrained by each model inform the models that follow.

4.1 Constant Eddington Ratio

A distribution of calculated Eddington ratios is shown in Figure 7.2. This is taken from the quasar properties catalog compiled by Shen et al. [21]. A peak for this sample from a best-fit PDF gives $\lambda = 0.18466$. It should be mentioned that this is not a flux-limited sample. There are implications to be considered here. A flux-limited sample would possibly be much more "complete" in the sense that it could be described as being representative of the entirety of the population. However, any flux limited sample would have a cut-off with respect to redshift and a cut-off with respect to luminosity. Since the Eddington ratio is likely a function of redshift, as considered by McLure & Dunlop [13] and Cao [2], this could potentially bias the sample to lower Eddington ratios. Any cut-off with respect to luminosity

could bias the sample to higher Eddington ratios. This analysis of Eddington ratios is not intended to be complete; it is only an attempt to constrain the value for fixed Eddington ratio models. For this model I have adopted the mean of this distribution, $\lambda = 0.263$.

The functional form for $\delta(M,t)$ is $\delta_0 e^{-t/\tau}\left(\frac{M}{M_\odot}\right)^{-\mu}$ and the values which give the most reasonable fit to the observed luminosity functions are, $\delta_0 = 0.1$, $\tau = 6 \times 10^9$ yrs., and $\mu = 0.02$. In solving this equation, I have taken the solar luminosity to be $L_\odot = 3.846 \times 10^{26}$ W, the solar mass to be $M_\odot = 1.99 \times 10^{30}$ kg.

A comparison of these results at different redshifts shows that while there is some agreement, there is a great deal of room for refinement. The luminosity function determined by this method is shown in Fig. 7.3. For comparison, the luminosity function determined by HRH07 is shown. It can be seen that there is significant disagreement at redshifts of 0.1 and 2.0. A plot of the mass functions at various redshifts for this model is shown in Fig. 7.4. This model has assumed a constant Eddington ratio; subsequent models will explore a variable Eddington ratio. This initial model gives a qualitative feel for the time evolution of these two functions (Fig. 7.5).

If instead, a local luminosity function is used as input and the same dynamics are applied, the results disagree at higher redshifts. Here the solutions are for Eq. 2.9 instead of Eq. 2.8. The results are shown in Figs. 7.6. The input luminosity function is the best-fit QLF at $z = 0.1$ from HRH07:

$$\Phi(L, 0.1) = \frac{10^{-5.45}}{\left(\frac{L}{10^{11.94} L_{\odot}}\right)^{0.868} + \left(\frac{L}{10^{11.94} L_{\odot}}\right)^{1.97}}.$$

4.2 Density vs. Luminosity Evolution

In order to shed some light on the effect of mass and time dependencies on the accretion rate parameters, I present two models which contrast these effects. In one model, the Eddington ratio depends on time and the duty cycle depends on mass. The other model supposes an Eddington ratio that decays with mass and a duty cycle decays that with time. I have modeled these with identical parameters so the the evolution of the mass functions is the same, however the difference between the luminosity functions is significant. The results are shown in Figures 7.8 and 7.9. It can be seen by comparing the luminosity functions for these that a time-dependent Eddington ratio contributes to luminosity evolution and a time-dependent duty cycle contributes to the density evolution. This is most evident in the luminosity function for the spiral AGN (Fig. 7.9).

4.3 Dark Accretion

This section considers an alternative model to those presented previously. The basis for this model is the idea that tidal disruption of in-falling stellar material is responsible for the

bulk of the luminosity of AGN. The implications of this idea are explored, and ultimately it is found that this is not a viable alternative to the widely accepted model of the accretion engine.

4.3.1 Diminished efficiency

Suppose that the primary mechanism for the AGN fueling is from tidal forces acting on the in-falling matter. The primary region in which this tidal disruption would occur would be within the Roche limit. As the black hole accretes matter, the event horizon would grow and eventually exceed the Roche limit. For a non-rotating black hole with stellar density material, this would be around $\log M/M_\odot = 8.7$. Perhaps the most straightforward way to represent this in terms of the accretion dynamics would be with an efficiency parameter that decreases at the break mass,

$$\epsilon = \epsilon_0 \left(1 - \frac{\sigma}{1 + e^{-\chi(\log M/M_B)}}\right) \tag{4.1}$$

where ϵ_0 is the maximum efficiency, σ is the fractional contribution of tidal forces to the accretion engine, and χ controls the transition at the break.

There are two important implications of this: since the efficiency parameter decreases, so then does the luminosity. The accretion then proceeds 'dark'. The other implication is that the accretion onto the black hole actually increases as a result, since matter/energy is no longer radiated out.

Additionally, it should be considered that the Eddington ratio is not a free parameter. Consider a black hole with matter in-falling at some fueling rate $\dot{M}_f$. This fueling rate is

not dependent on the activity within the accretion disk (ignoring feedback). This is related to the accretion rate by

$$\dot{M}_f = \frac{\dot{M}}{(1-\epsilon)} \tag{4.2}$$

so the Eddington ratio becomes

$$\lambda = \frac{\epsilon \dot{M}_f t_E}{M}. \tag{4.3}$$

The Eddington ratio must then be a function of the efficiency parameter, which is itself likely a function of mass. Now since the luminosity function can be found from the mass function by

$$\Phi(L,t) = N(M,t)_{M=Lt_E/\lambda c^2}$$

and the Eddington ratio is a function of mass, this leads to a transcendental equation for the chosen form for ϵ and for fueling rates that are mass-dependent. Solutions may be found for the mass function, but not for the luminosity function.

4.3.2 Accretion without radiation

Another approach which avoids this problem is to incorporate the tidal disruption into the duty cycle. The duty cycle was defined as the probability that a particular black hole would be accreting at a given time. If we modify this interpretation in consideration of this 'dark' accretion model, it could be thought of as the probability that a black hole would be luminous at a given time, however it may still be accreting. Modeling the duty cycle in the

same manner as the efficiency parameter:

$$\delta = \delta_0 \left(1 - \frac{\sigma}{1 + e^{-\chi(\log M/M_B)}}\right) \tag{4.4}$$

This can be implemented by solving Eq. 2.8 with a slight modification:

$$-\frac{2H_0}{3}(1+z)^{5/2}\frac{\partial N}{\partial z} + \frac{\lambda(1-\epsilon)}{\epsilon t_E \ln 10}\frac{\partial N}{\partial \log M/M_\odot} = S(M,z) \tag{4.5}$$

Notice that the duty cycle does not appear in the accretion coefficient this time. The luminosity function can then be extracted in the same manner as before: from Eq. 2.10. The chosen form for the Eddington ratio for this model is $\lambda = \lambda_0 e^{-t/\tau}$ and the duty cycle has the form given in Eq. 4.4 with an exponential time-dependency as well.

The result of this is that mass is accreted much faster. Since accretion is not limited by the duty cycle, the resulting mass and luminosity functions are not consistent with observed mass and luminosity functions. This model can be matched to observations by adopting an efficiency parameter $\epsilon = 0.9$, which is physically unrealistic. The results of this model are shown in Figs. 7.10 and 7.11. It would seem then that the contribution of tidally disruptive 'dark' accretion is negligible.

4.4 Break in Duty Cycle

Next I will take a look at a model that uses the duty cycle developed in the previous section. The duty cycle there is relatively flat, then breaks at some mass, dropping to nearly zero. In this model, the results of which are shown in Figs. 7.12 and 7.13, I have used an input mass

function that is a single power law at redshift $z = 5$. Of note is the fact that the break in the duty cycle here is responsible for introducing a break in the mass function and luminosity functions. It is possible that the break in observed luminosity functions is caused by this break in the duty cycle which is itself possibly caused by feedback [22].

Taking the same dynamics from Model 3 and using an input local mass function, the evolved luminosity function can be fitted closely to the observed luminosity function as shown in Fig. 7.18. The evolved mass function for this model is shown in Fig. 7.19. This model seems to be the most reasonable in terms of matching the observed mass and luminosity functions.

5 Discretized Modeling

The models discussed up to now have been developed using the continuity equation. This essentially represents the populations as continuous functions and is computationally expedient for modeling a large number of objects. This chapter is devoted to the discussion of a model where the objects are modeled individually and evolved through time in a probabilistic manner dictated by the duty cycle.

5.1 Algorithm

The population is established with pseudorandom masses distributed according to the mass function from SWM09 at $z = 5$. The masses then evolve iteratively through time, where at each iteration the probability of accretion is determined by the duty cycle. When accretion occurs, it is determined by $\dot{M}\Delta t$ where Δt is the time step for the iteration. At the end of a redshift interval, the luminosity function is calculated from the black holes that accreted at the last iteration. This is then repeated for each redshift interval.

5.2 Implications

This has two advantages over the previous method. First, it requires no artificial boundary conditions. Second, it is relatively straightforward to introduce the effect of mergers without propagating the entire population to lower number densities. For comparison, the results of this model are presented with no mergers (5a), 'dark' mergers (5b), and mergers that result in an increase in luminosity (5c). The modeling of mergers in this fashion is somewhat primitive. For this model I chose the probability of a merger per Gyr. to be 0.4 for an individual black

hole. This probability is somewhat exaggerated simply to illustrate the qualitative effect of mergers. For Model 5c, where the mergers produce an increase in luminosity, this was implemented by introducing an efficiency parameter η that represents the fraction of the merging body mass that contributes to the luminosity during the merger. For this case I chose $\eta = 0.2$. This model is not intended to be comprehensive, and it requires further study. This model is introduced and the results are presented to illustrate the effect of mergers. The luminosity and mass functions of these models are shown in Figs. 7.20 - 7.25.

It should be pointed out that the parameters for accretion in Model 5 differ from those in Model 4. Each was chosen to provide a best fit to the observed luminosity function. They differ because they rely on different input mass functions: Model 4 has the MF from SWM09 at $z = 0.02$ and Model 5 has a single power law fitted to the mass function from SWM09 at $z = 5$. Model 4 fits the observed luminosity functions fairly well; Model 5a fits the observed luminosity functions at higher luminosities, and fits the mass functions from SWM09 as well.

One consequence of this approach is that it forces special attention to be paid to the low mass end of the function. With this approach, the bulk of the objects are in that regime, so the shape of the function becomes important at the low mass/luminosity end. These objects contribute greatly to the evolution of the mass/luminosity function. However, this presents difficulties in implementation since computation time depends directly on the number of objects modeled. To balance this, I have restricted the objects to $\log M/M_{\odot} > 2$. The total number of objects used in the starting sample was 1,040,921, and it was run with 10 iterations per unit redshift.

6 Conclusion

The results presented herein indicate that any model based on a tidal disruption of infalling material is untenable given the dynamics assumed here. Additionally the agreement between observed and derived mass and luminosity functions for models with a duty cycle with a break with mass seem to indicate that there is some mechanism responsible for the break, and it is most likely a result of feedback. Discretized models seem to indicate that mergers cause a mass evolution, as expected, and any model incorporating mergers may imply a lower Eddington ratio to match observed luminosity functions (though this was not explored in this research).

6.1 Spiral AGN functions

Much of the discussion up to this point has dealt with the comparison between the complete luminosity functions and the luminosity functions derived in the models developed herein. It would be useful at this point to discuss the spiral galaxy mass and luminosity functions.

First, the evolution of the spiral AGN luminosity function provides a constraint on the dynamics in general. Any dynamics that allow a luminosity function for spiral AGN to exceed that of the AGN population as a whole are not viable and so set constraints on allowed dynamics.

Another point worth mentioning, as pointed out in Section 4.2, the peak of the spiral AGN luminosity function can be used to surmise density evolution or luminosity evolution. The propagation of the peak in the spiral AGN function is more obvious than the propagation of the break in a double power law luminosity function. It should be pointed out however,

that the peak may be artificial. It is likely that the low mass end of the spiral SMBH mass function is underestimated [5]. It is possible that with more estimates of the low mass end of this function, it may turn out to have a double power law shape. It should be mentioned again that the dynamics applied to the spiral AGN in this research are the same dynamics applied to the complete AGN population This work assumes that the dynamics that govern black holes in spiral galaxies are the same as those found in early-type galaxies.

Bibliography

[1] Ade, P. A. R., et al. "Planck 2013 results. XVI. Cosmological parameters." *Astronomy & Astrophysics* 571 (2014): A16.

[2] Cao, Xinwu. "Cosmological evolution of massive black holes: Effects of Eddington ratio distribution and quasar lifetime." *The Astrophysical Journal* 725.1 (2010): 388.

[3] Cavaliere, A., P. Morrison, and K. Wood. "On Quasar Evolution." *The Astrophysical Journal* 170 (1971): 223.

[4] Cavaliere, A., et al. "Quasar evolution and Gravitational Collapse." *The Astrophysical Journal* 269 (1983): 57-72.

[5] Davis, Benjamin L., et al. "The black hole mass function derived from local spiral galaxies." *arXiv preprint arXiv:1405.5876* (2014).

[6] Ferrarese, Laura, and David Merritt. "A fundamental relation between supermassive black holes and their host galaxies." *The Astrophysical Journal Letters* 539.1 (2000): L9.

[7] Gebhardt, Karl, et al. "A relationship between nuclear black hole mass and galaxy velocity dispersion." *The Astrophysical Journal Letters* 539.1 (2000): L13.

[8] Häring, Nadine. "On the black hole mass-bulge mass relation." *The Astrophysical Journal Letters* 604.2 (2004): L89.

[9] Hartle, James B. *Gravity: An Introduction to Einstein's General Relativity.* San: Francisco: Addison Wesley, 2003. Print.

[10] Hopkins, Philip F., Gordon T. Richards, and Lars Hernquist. "An observational determination of the bolometric quasar luminosity function." *The Astrophysical Journal* 654.2 (2007): 731.

[11] Kollmeier, Juna A., et al. "Black hole masses and Eddington ratios at $0.3 < z < 4$." *The Astrophysical Journal* 648.1 (2006): 128.

[12] Macdonald, Alan. "Comment on "The Cosmic Time in Terms of the Redshift", by Carmeli et al." *arXiv preprint gr-qc/0606038* (2008).

[13] McLure, Ross J., and James S. Dunlop. "The cosmological evolution of quasar black hole masses." *Monthly Notices of the Royal Astronomical Society* 352.4 (2004): 1390-1404.

[14] Peterson, Bradley M. *An Introduction to Active Galactic Nuclei.* Cambridge: Cambridge University Press, 1997. Print.

[15] Salpeter, E. E. "Accretion of interstellar matter by massive objects." *The Astrophysical Journal* 140 (1964): 796-800.

[16] Schmidt, Maarten. "3C 273: a star-like object with large red-shift." *Nature* 197.4872 (1963): 1040.

[17] Schmidt, Maarten. "Space distribution and luminosity functions of quasi-stellar radio sources." *The Astrophysical Journal* 151 (1968): 393.

[18] Shankar, Francesco, David H. Weinberg, and Jordi Miralda-Escudé. "Self-consistent models of the AGN and black hole populations: duty cycles, accretion rates, and the mean radiative efficiency." *The Astrophysical Journal* 690.1 (2009): 20.

[19] Shankar, Francesco, David H. Weinberg, and Jordi Miralda-Escudé. "Accretion-driven evolution of black holes: Eddington ratios, duty cycles, and active galaxy fractions. " *Monthly Notices of the Royal Astronomical Society* (2012).

[20] Shapiro, Stuart L. "Spin, accretion, and the cosmological growth of supermassive black holes." *The Astrophysical Journal* 620.1 (2005): 59.

[21] Shen, Yue, et al. "A catalog of quasar properties from Sloan Digital Sky Survey release 7." *The Astrophysical Journal Supplement Series* 194.2 (2011): 45.

[22] Silk, Joseph, and Martin J. Rees. "Quasars and galaxy formation." *arXiv preprint astro-ph/9801013* (1998).

[23] Small, Todd A., and Roger D. Blandford. "Quasar evolution and the growth of black holes." *Monthly Notices of the Royal Astronomical Society* 259.4 (1992): 725-737.

7 Appendix

7.1 Cosmology

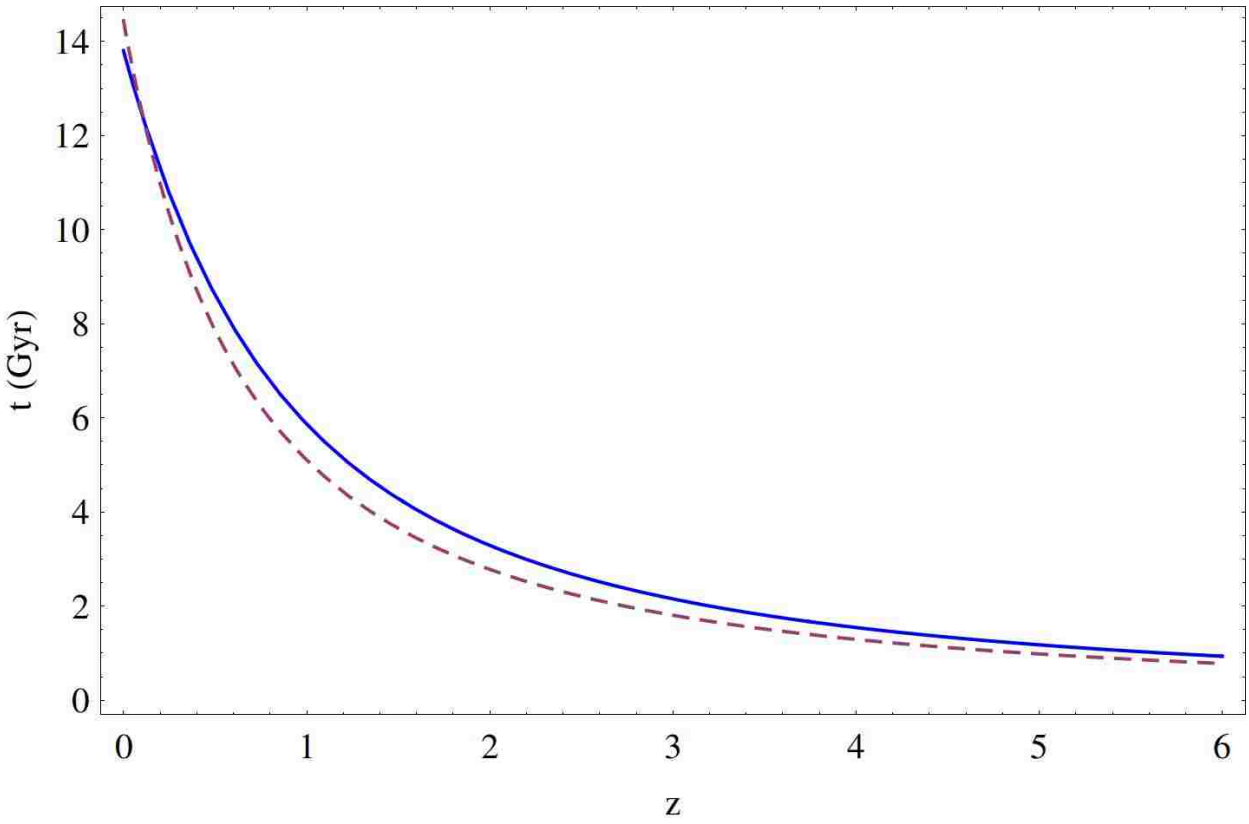

Figure 7.1: Comparison between redshift-time relation from Eq. 7.1 [12] shown as solid line and approximation used in Eq. 2.7 (dashed line).

Here the time as a function of redshift is taken to be

$$t(z) = \frac{2H_0^{-1}}{3\Omega_\Lambda^{1/2}} \sinh^{-1}\left[\left(\frac{\Omega_\Lambda}{\Omega_M}\right)^{1/2}(z+1)^{-3/2}\right]. \tag{7.1}$$

This approximation is valid over the range of redshifts used in this research, and is used as a means of simplifying the forms of differential equations being solved numerically.

7.2 Tables and Figures

	δ	λ	ϵ	Input B. C.
1a	$\delta_0 e^{-t/\tau}\left(\frac{M}{M_\odot}\right)^{-\mu}$	0.262951	0.1	SWM09 at $z = 0.02$
1b	$\delta_0 e^{-t/\tau}\left(\frac{M}{M_\odot}\right)^{-\mu}$	0.262951	0.1	HRH07 at $z = 0.1$
2a	$\delta_0\left(\frac{M}{M_\odot}\right)^{-\mu}$	$\lambda_0 e^{-t/\tau}$	0.1	SWM09 at $z = 0.02$
2b	$\delta_0 e^{-t/\tau}$	$\lambda_0\left(\frac{M}{M_\odot}\right)^{-\mu}$	0.1	SWM09 at $z = 0.02$
Dark	$\delta_0\left(1-\frac{\sigma}{1+e^{-\chi(\log M/M_B)}}\right)e^{-t/(8.7\times10^{10}\text{ yrs.})}$	$\lambda_0 e^{-t/\tau}$	0.9	SWM09 at $z = 0.02$
3	$\delta_0\left(1-\frac{\sigma}{1+e^{-\chi(\log M/M_B)}}\right)e^{-t/(3\times10^{9}\text{ yrs.})}$	$\lambda_0 e^{-t/\tau}$	0.1	$\frac{10^{1.304}}{(M/M_\odot)^{0.761}}$ at $z = 5$
4	$\delta_0\left(1-\frac{\sigma}{1+e^{-\chi(\log M/M_B)}}\right)e^{-t/(5.0\times10^{9}\text{ yrs.})}$	$\lambda_0 e^{-t/\tau}$	0.1	SWM09 at $z = 0.02$
5	$\delta_0\left(1-\frac{\sigma}{1+e^{-\chi(\log M/M_B)}}\right)e^{-t/(5.0\times10^{9}\text{ yrs.})}$	$\lambda_0 e^{-t/\tau}$	0.1	SWM09 at z = 5.0

Table 7.1: A summary of the properties of the models presented herein. Note models 2a and 2b were have the same dynamical parameters, but the dependencies of the Eddington ratio and duty cycle on mass and time are switched for comparison.

	δ_0	λ_0	τ	μ	χ	σ	M_b
1a	0.1	X	6×10^9 yrs.	0.02	X	X	X
1b	0.1	X	6×10^9 yrs.	0.02	X	X	X
2a	0.08	2.0	2.2×10^9 yrs.	0.05	X	X	X
2b	0.08	2.0	2.2×10^9 yrs.	0.05	X	X	X
Dark	0.02	0.65	4.5×10^9	X	0.8	0.9	9.1
3	0.6	0.44	5.64×10^9 yrs.	X	1.61	1	9.1
4	0.50	0.58	4.2×10^9 yrs.	X	2.9	0.88	8.7
5	0.50	0.58	4.2×10^9 yrs.	X	2.9	0.88	8.7

Table 7.2: The parameters chosen for the models as given in table 7.1. These parameters are chosen that give reasonable agreement with observed luminosity functions at all redshifts.

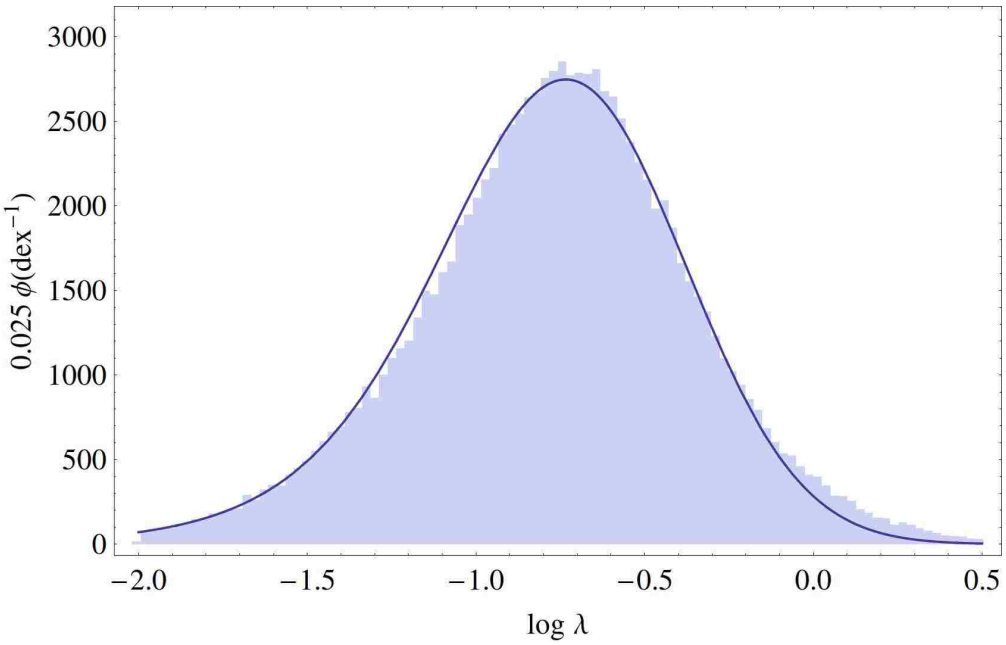

Figure 7.2: Logarithmic distribution of the Eddington ratio for a sample of quasars. The peak is at $\lambda = 0.18466$. The mean value of this sample is $\lambda = 0.262951$.

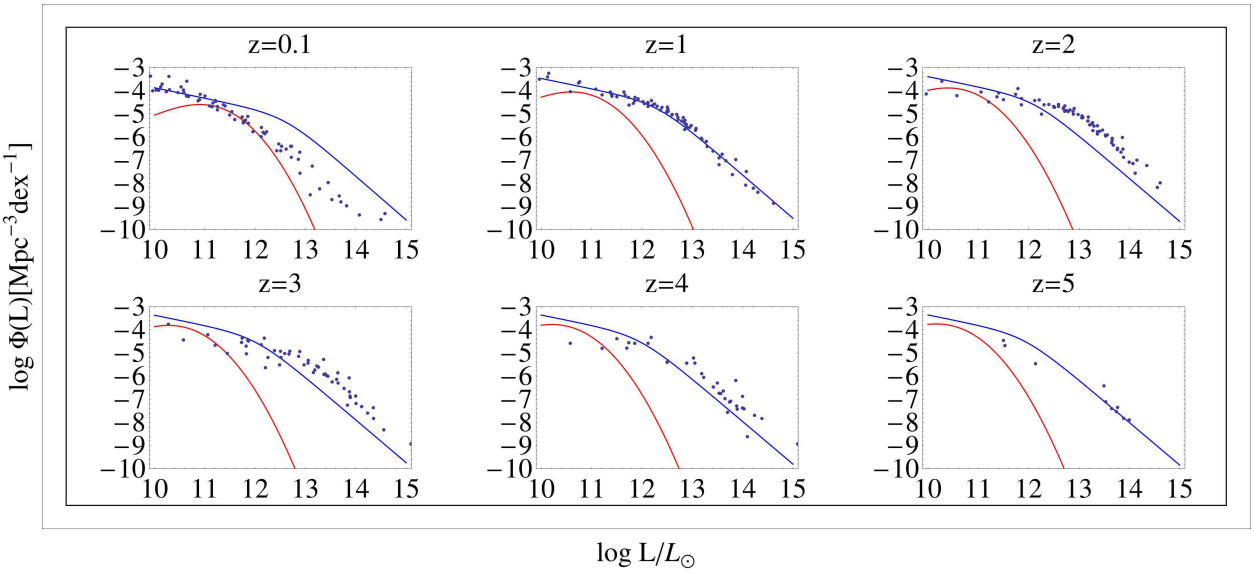

Figure 7.3: The luminosity function for Model 1a at various redshifts shown in blue. The spiral AGN luminosity function is shown in red. For comparison the observed luminosity function from HRH07 is plotted as blue dots. This is taken from the complete set of observations.

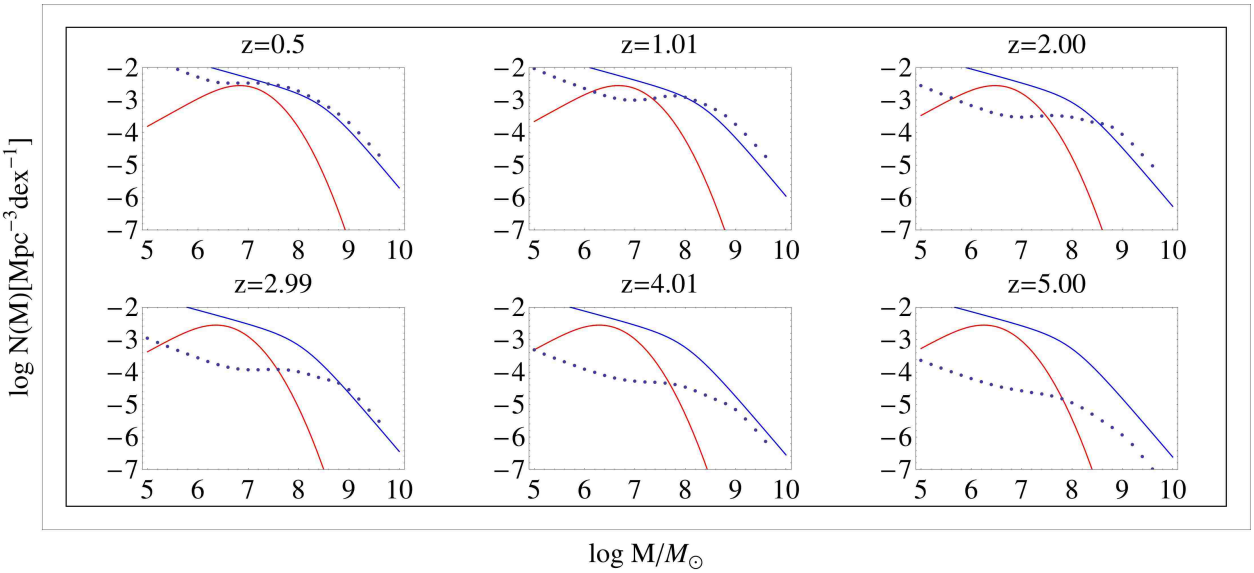

Figure 7.4: The mass functions for Model 1a at various redshifts shown in blue. The spiral AGN mass function is in red. The dots are calculated mass functions at the corresponding redshifts from SWM09.

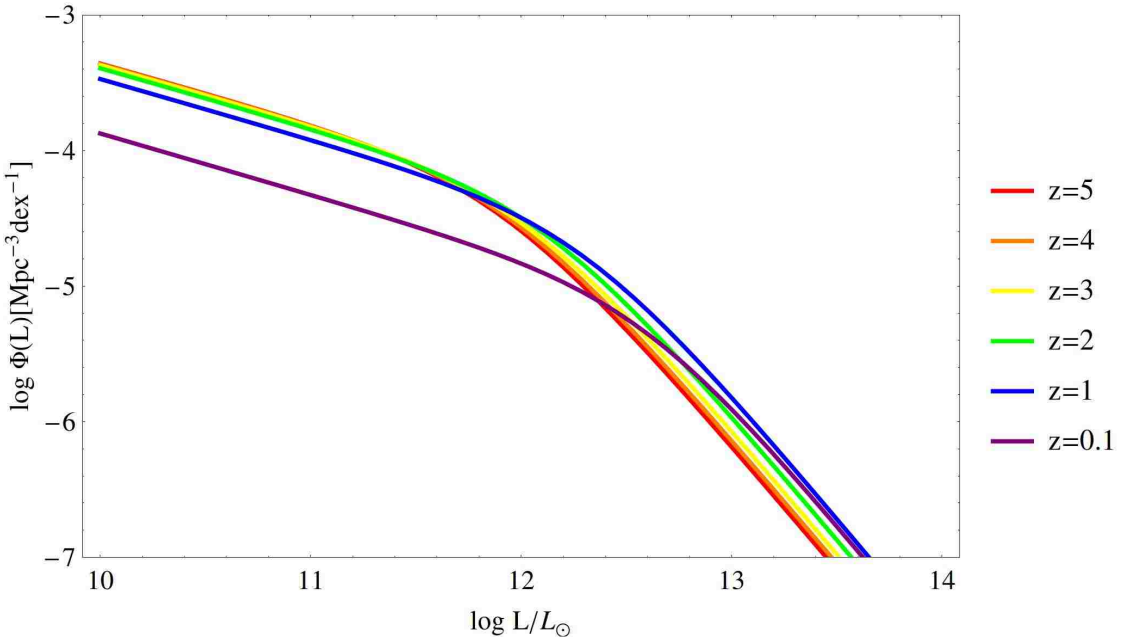

Figure 7.5: The luminosity function for Model 1a at various redshifts (blue curves from Fig. 7.3 shown here on single plot). This model exhibits both luminosity and density evolution as evidenced by the movement of the break.

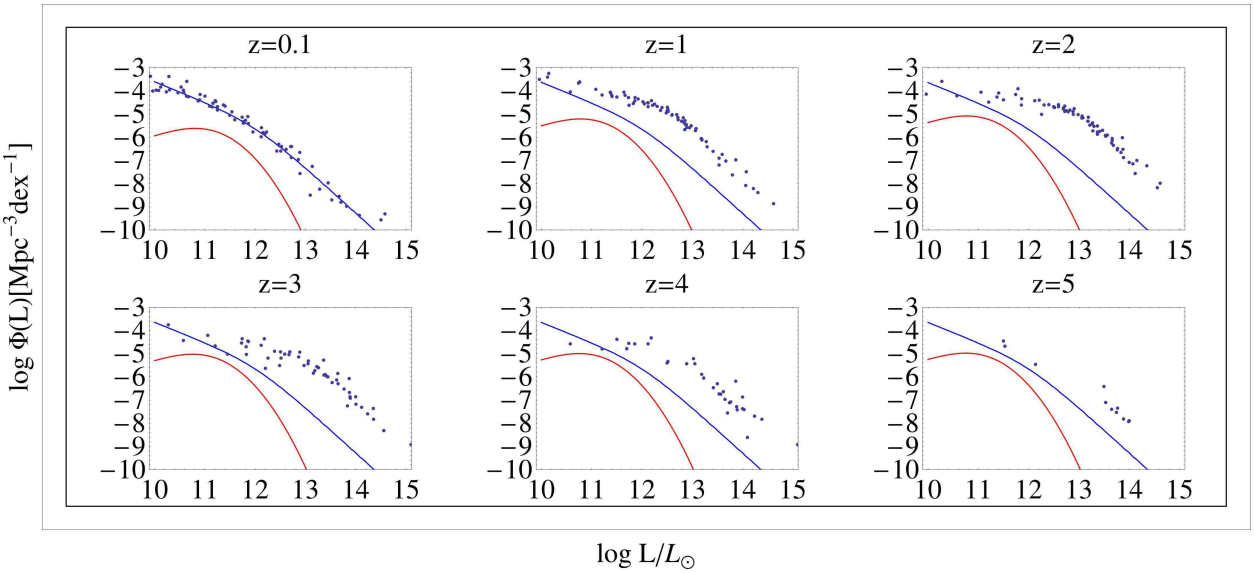

Figure 7.6: The luminosity function for Model 1b at various redshifts shown in blue. The spiral AGN luminosity function is shown in red. The observed luminosity function from HRH07 is shown for comparison.

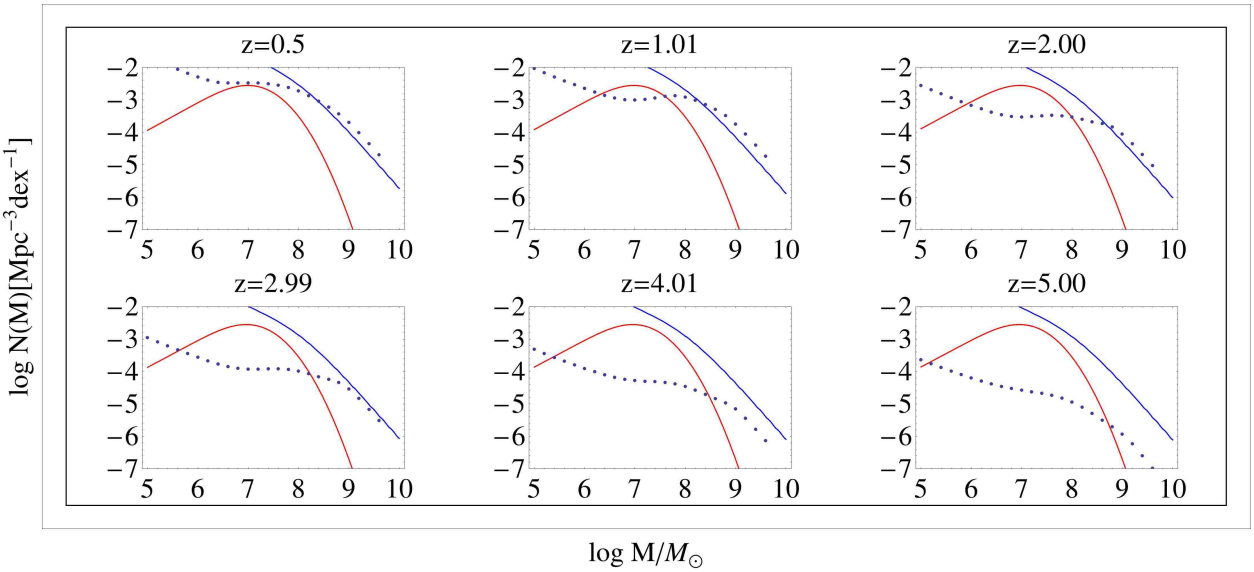

Figure 7.7: The mass functions for Model 1b at various redshifts shown in blue. The spiral AGN mass function is in red. The dots are calculated mass functions at the corresponding redshifts from SWM09.

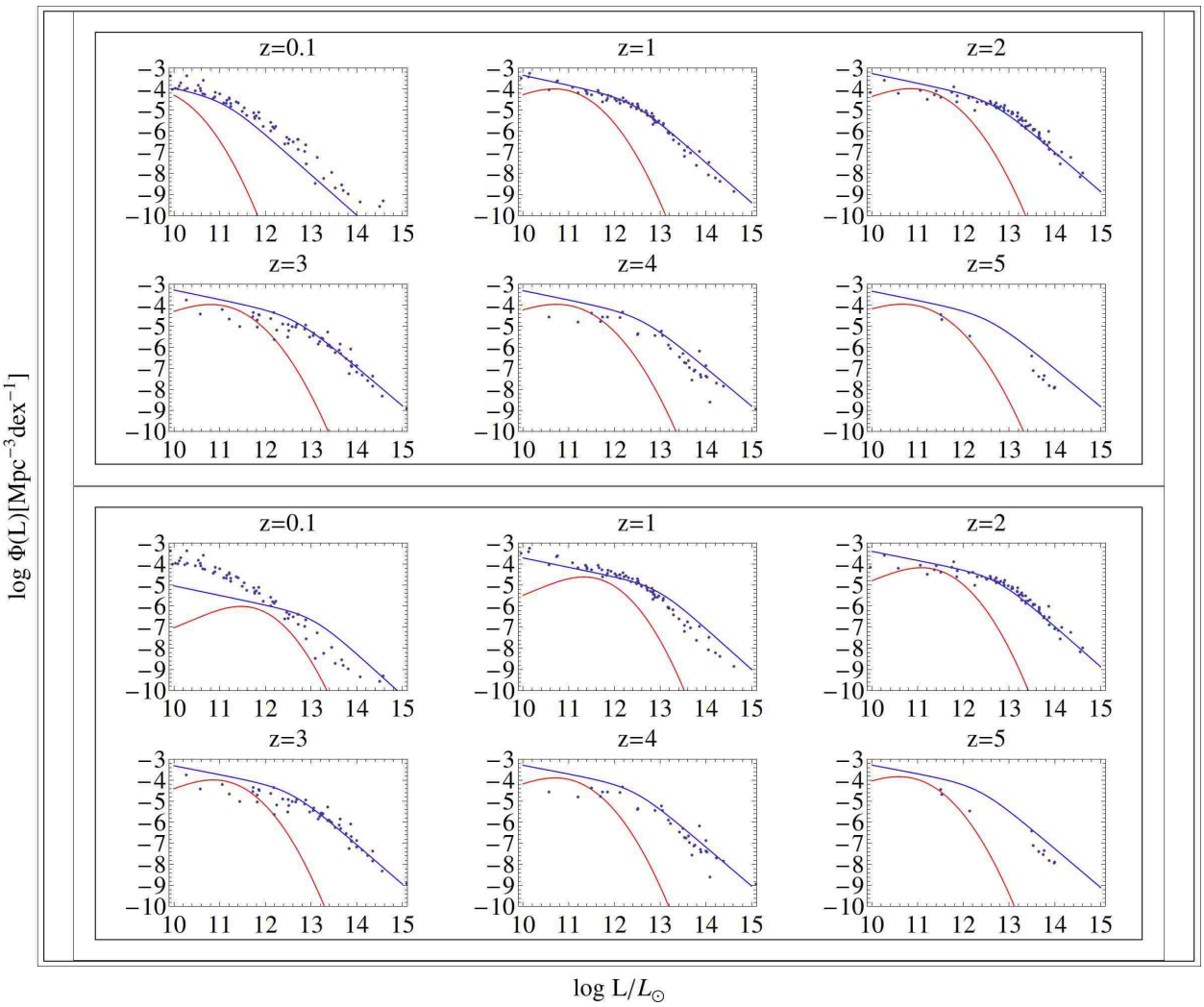

Figure 7.8: Comparison of luminosity functions for Models 2a (top) and 2b (bottom). Blue lines are the total luminosity functions for this model. Red lines are the spiral AGN luminosity functions. Blue dots indicate the luminosity functions taken from HRH07. The mass functions are not shown here since they are identical for both models. The luminosity functions are the same for redshifts $2 < z < 5$, however, they begin to show disagreement at $z < 2$.

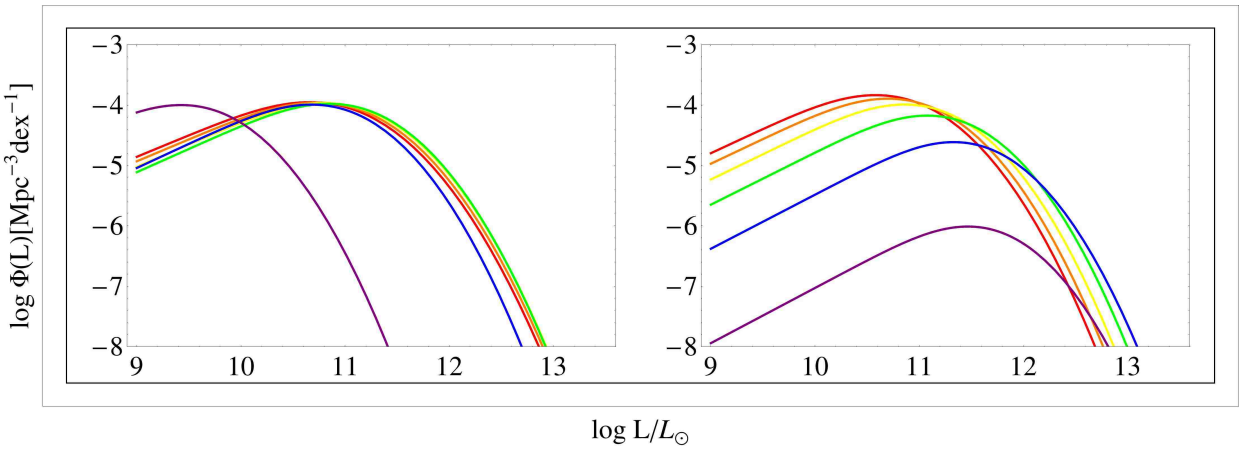

Figure 7.9: The spiral AGN luminosity function for Models 2a and 2b. Purple denotes redshift 0.1, blue: redshift 1, green: redshift 2, orange: redshift 3, yellow: redshift 4, red: redshift 5. Notice that model 2a on the left exhibits purely luminosity evolution, as would be expected with a time-varying Eddington ratio. Model 2b on the right exhibits mostly density evolution, as would be expected with a time-varying duty cycle.

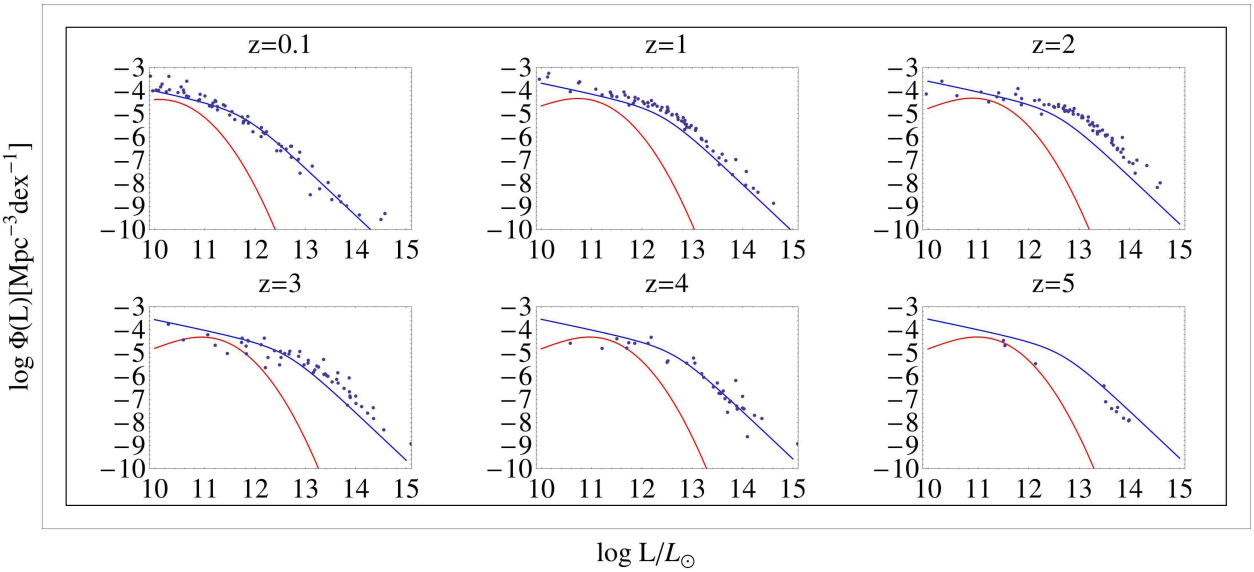

Figure 7.10: Luminosity function of the 'dark accretion' model at various redshifts. The blue line is the LF for the entire AGN population, the red line is the spiral AGN LF. Shown for comparison (blue dots) is the observed LF from HRH07. The results shown here depend on an efficiency parameter $\epsilon = 0.9$. Such a high efficiency parameter renders this model physically unrealistic.

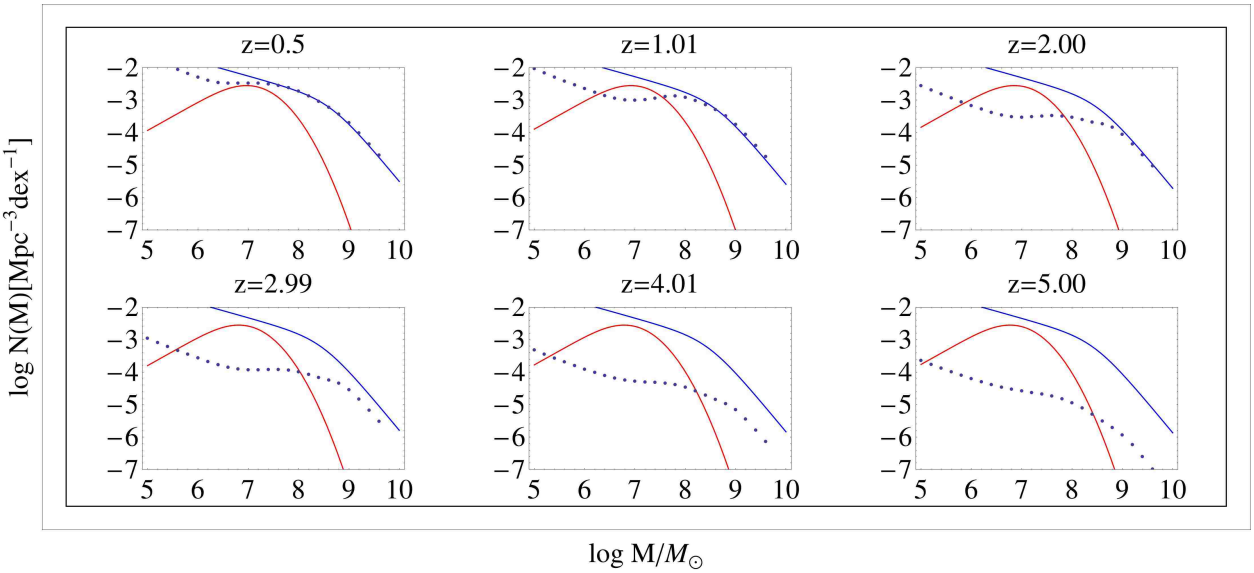

Figure 7.11: Mass function of the 'dark accretion' model for spiral galaxy SMBH (red) and the total BHMF (blue). Shown with the calculated mass functions from SWM09 (blue dots).

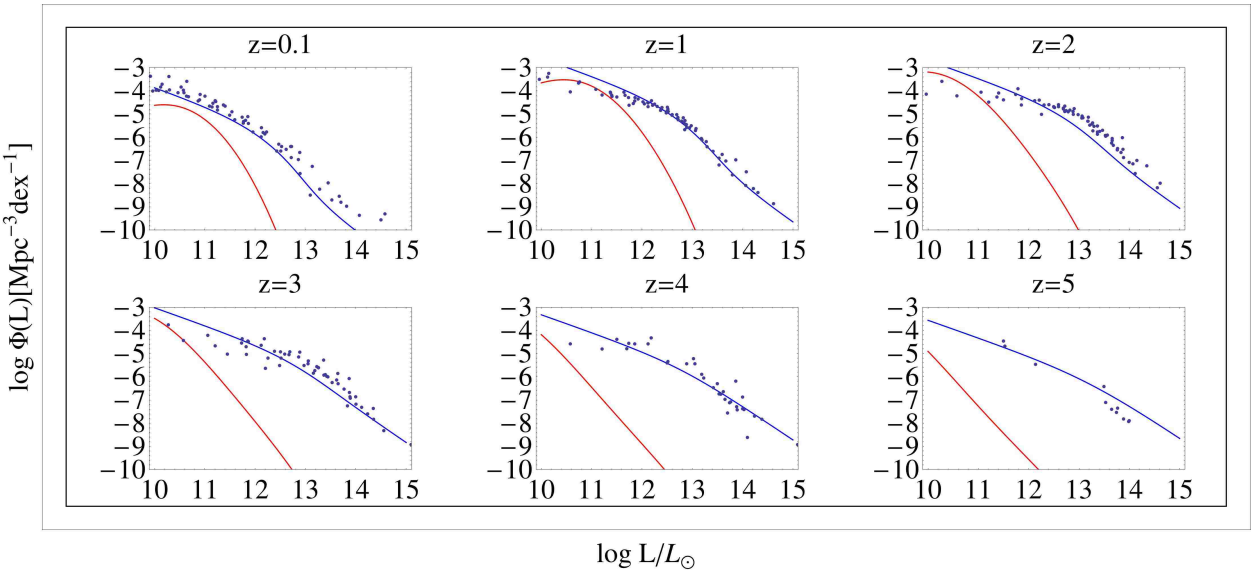

Figure 7.12: The luminosity function for Model 3 (blue line) with a single power law input mass function at $z = 5$. The red line is the spiral AGN LF. Blue dots are the observed LF from HRH07 using the complete set of observations. The break in the duty cycle induces a break in the luminosity function here giving it a double power law line-shape at lower redshifts.

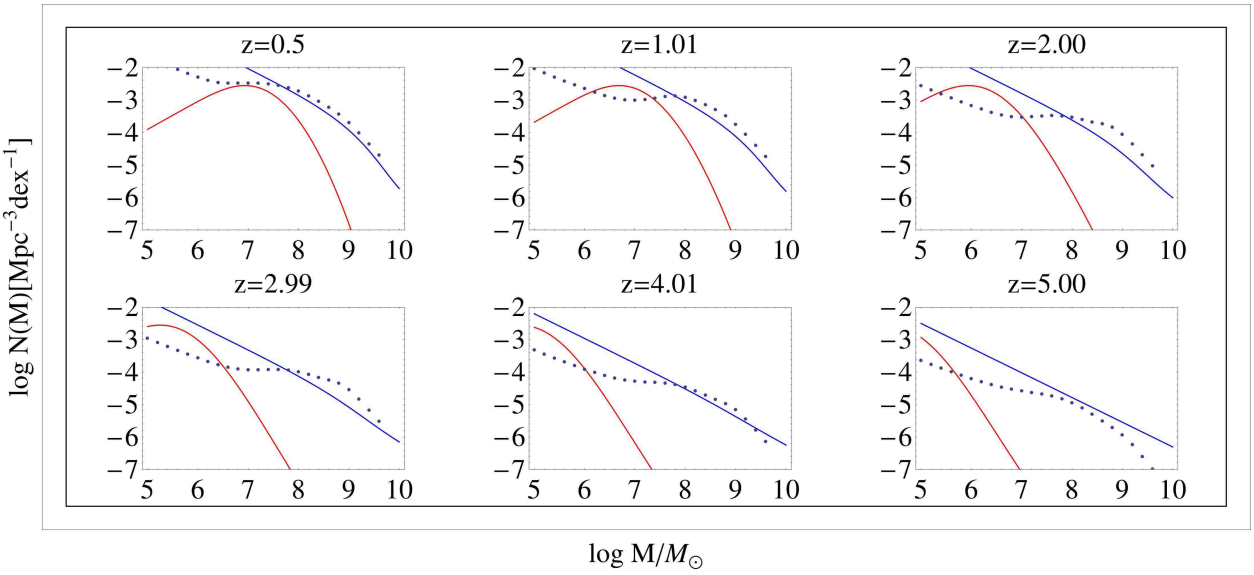

Figure 7.13: Mass function for Model 3, with single power law input mass function at $z = 5$. The input mass function is that shown in the bottom right frame. Notice that as the mass function evolves with time, a break is introduced around $\log M/M_\odot \sim 9$. This is caused by the break in the duty cycle around the same mass.

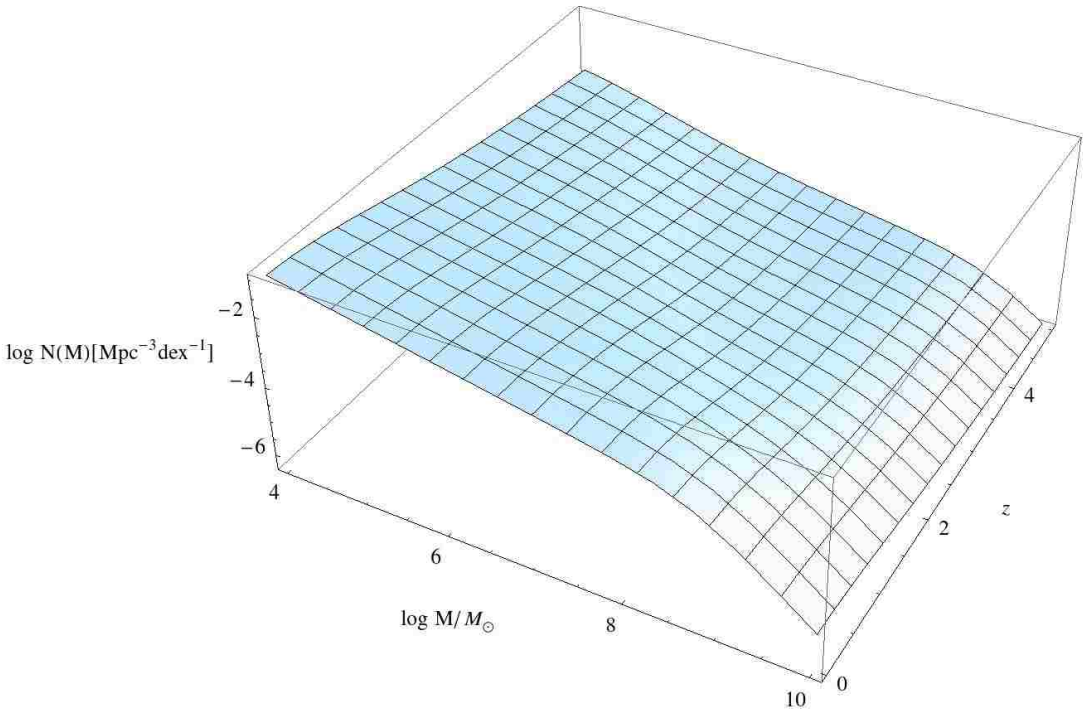

Figure 7.14: Complete mass function for Model 4 plotted as a function of mass and redshift. The time evolution of the break in the mass function can be seen qualitatively here.

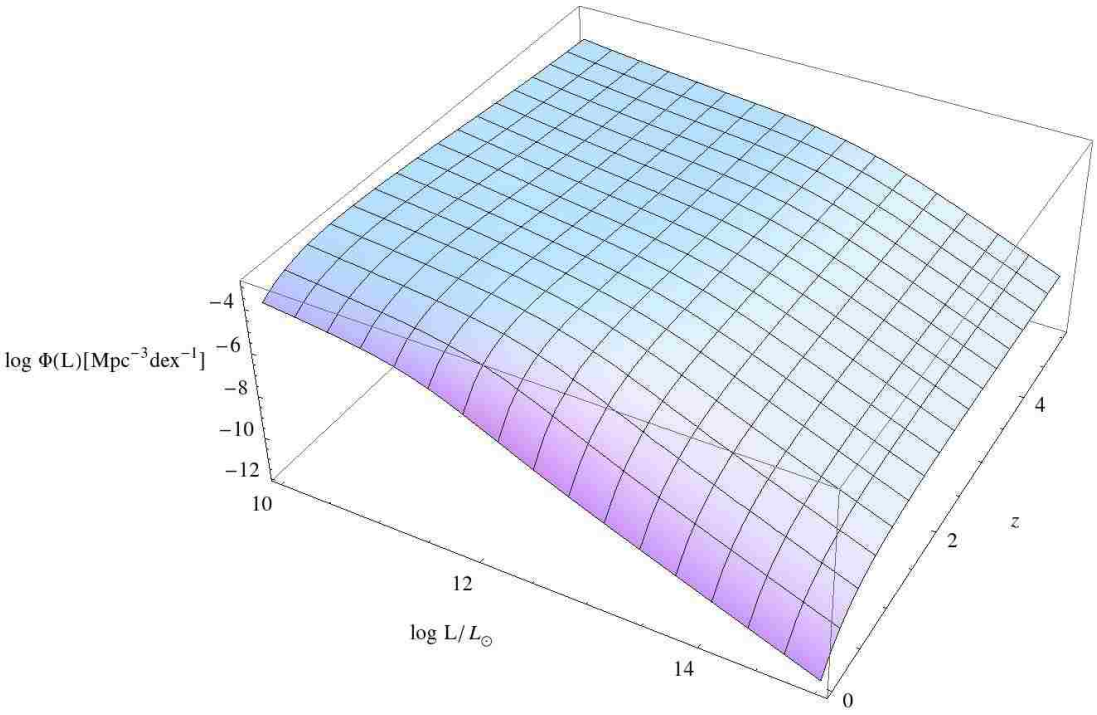

Figure 7.15: Complete bolometric luminosity function for Model 4 as a function of redshift.

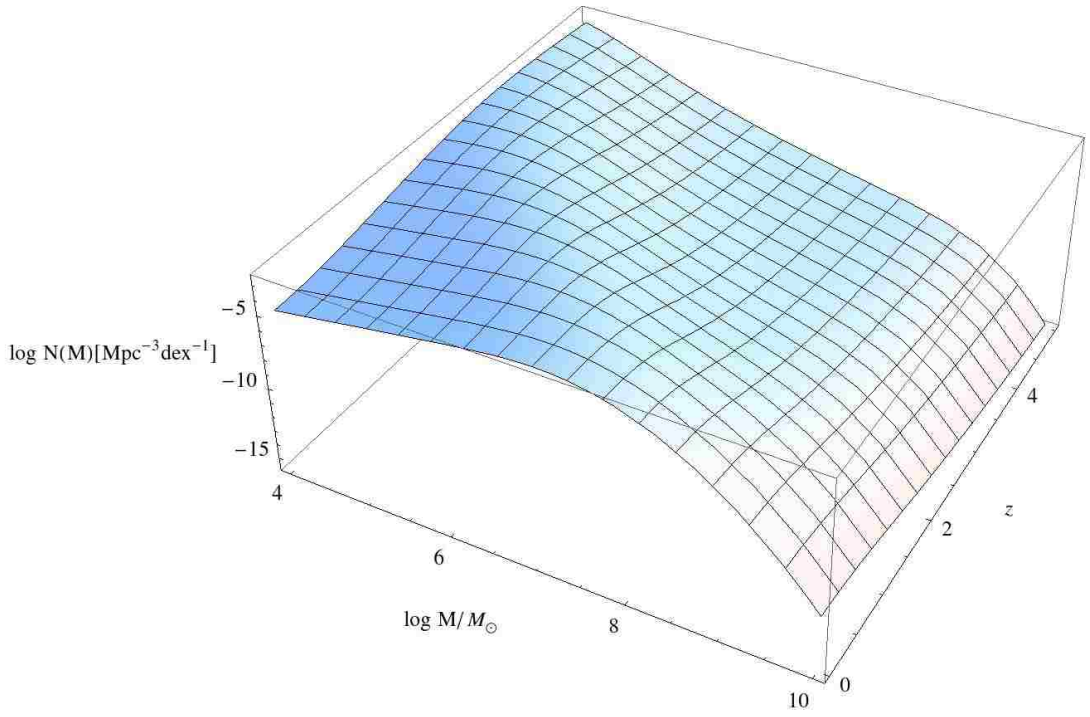

Figure 7.16: Mass function for spiral galaxies for Model 4.

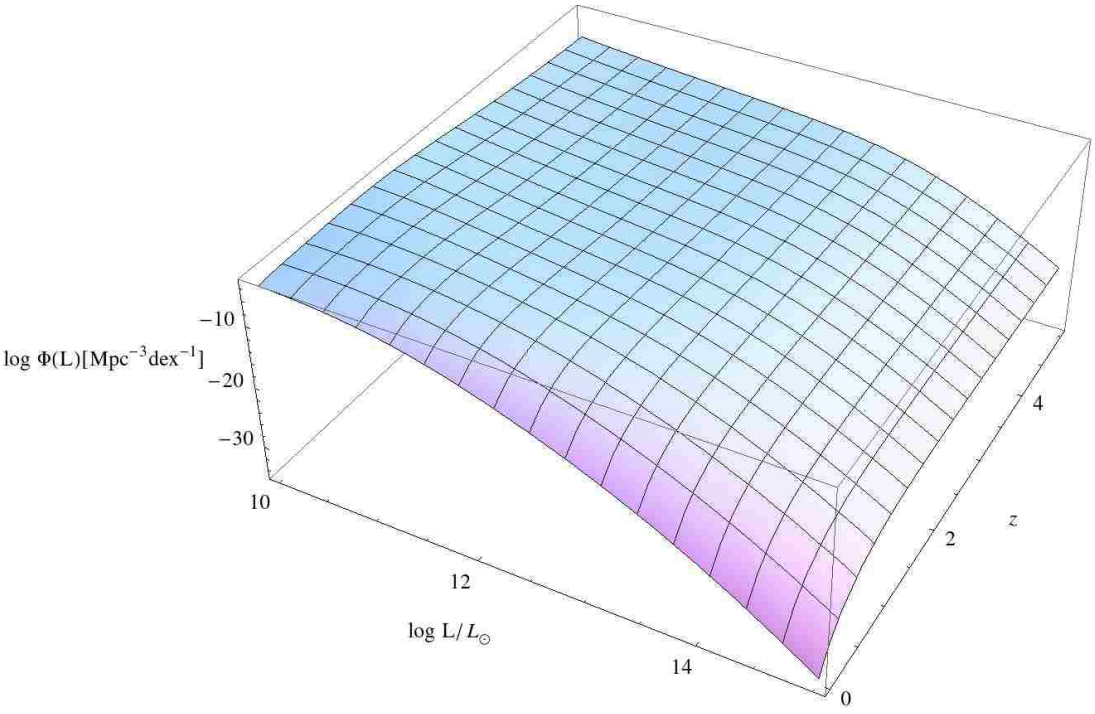

Figure 7.17: Luminosity function for spiral AGN for Model 4.

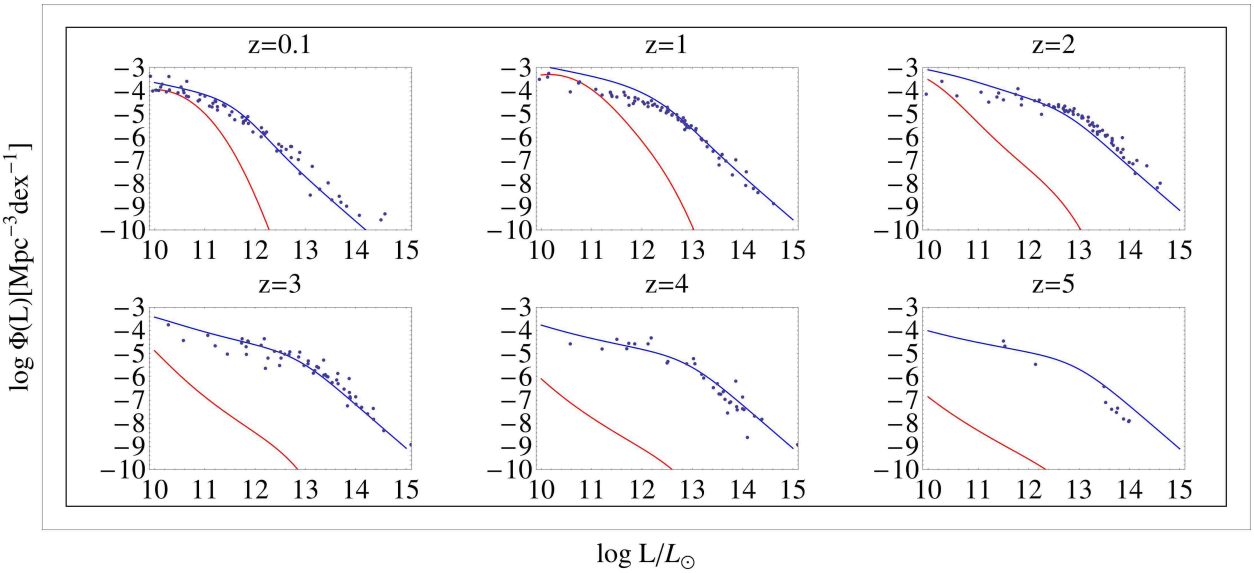

Figure 7.18: Complete luminosity function (blue) and the spiral AGN luminosity function (red) computed from Model 4 plotted at various redshifts.

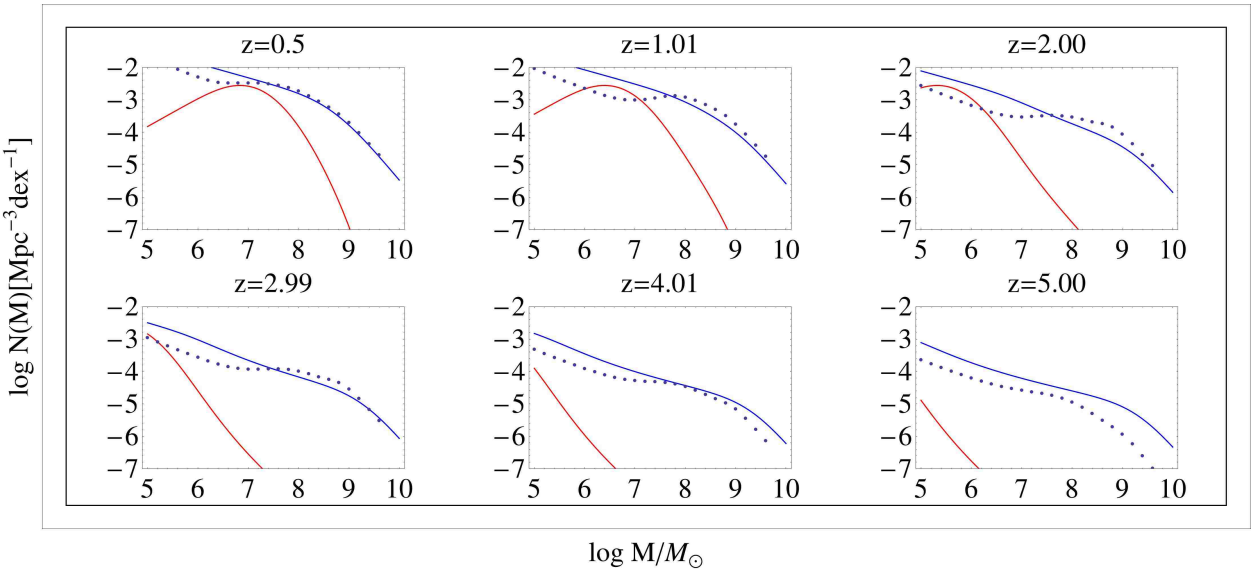

Figure 7.19: Complete mass function and spiral galaxy black hole mass function from Model 4 shown at various redshifts. Red line is the spiral BHMF, blue line is the total BHMF. Blue dots are BHMF estimates from SWM09.

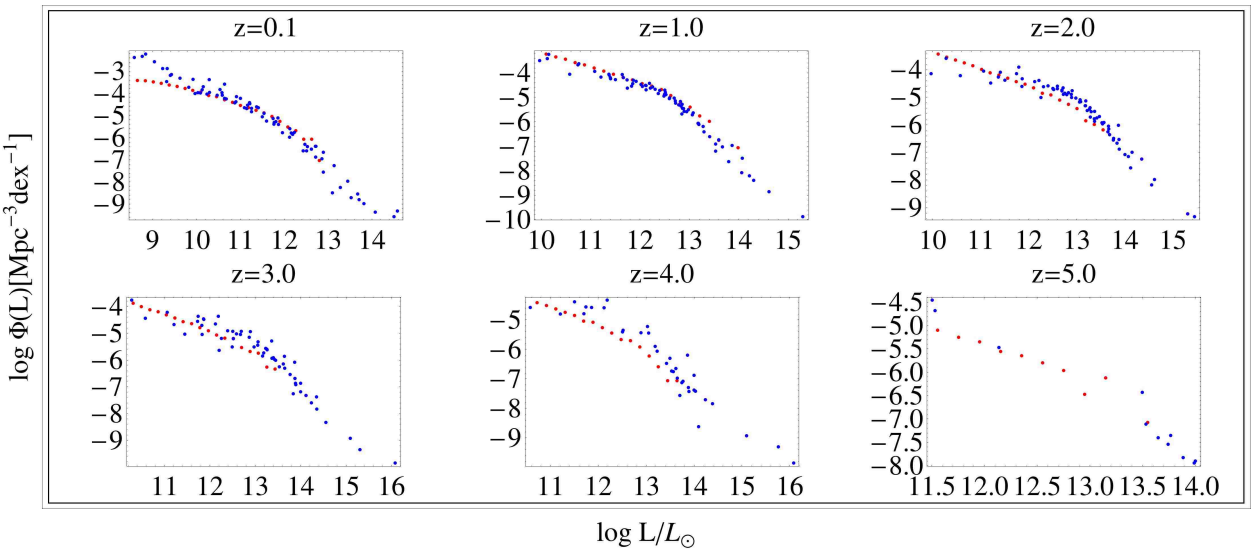

Figure 7.20: Luminosity function of Model 5a shown at various redshifts in red. Comparison with HRH07 shown in blue. Axes are not scaled the same for each plot.

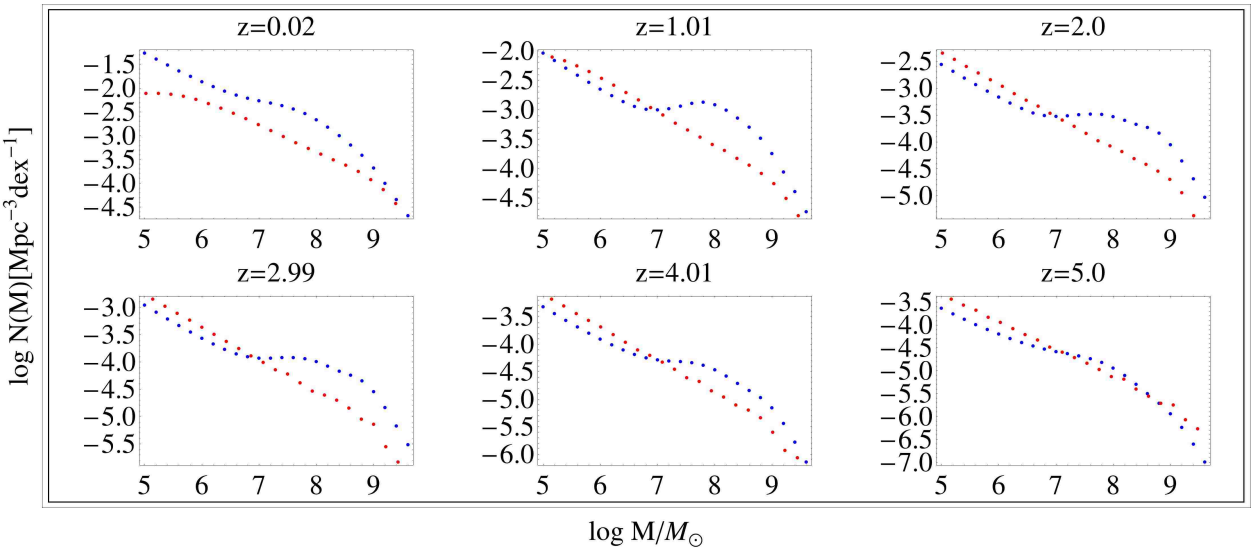

Figure 7.21: Mass function of Model 5a shown at various redshifts in red and calculated mass function from SWM09 shown in blue. Axes are not scaled the same for each plot.

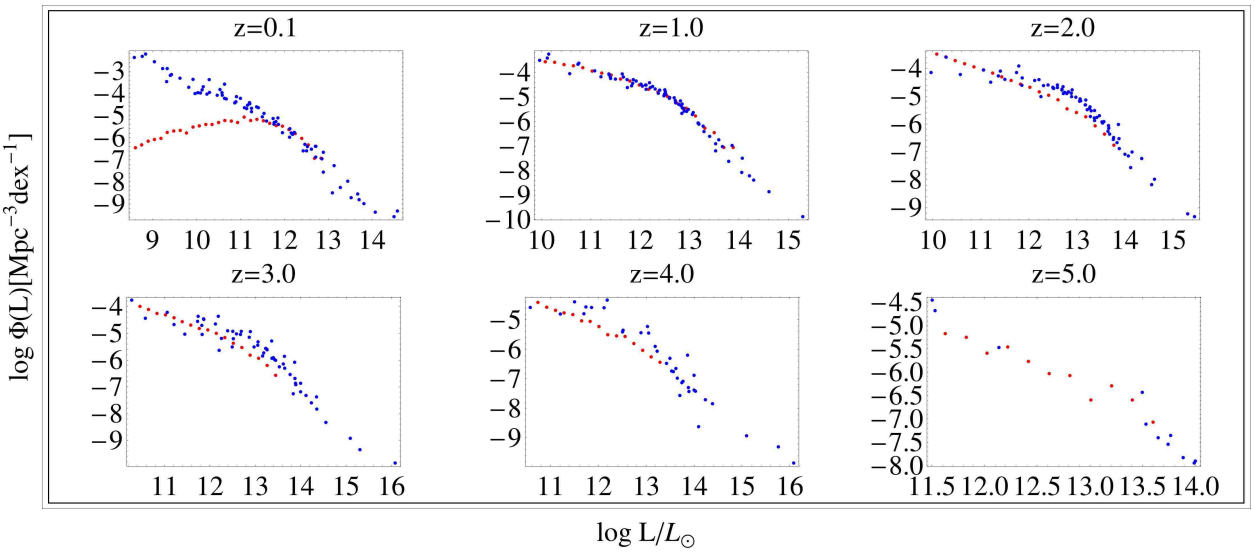

Figure 7.22: Luminosity function of Model 5b (red) including the effect of mergers on population. Comparison with HRH07 shown in blue. Axes are not scaled the same for each plot.

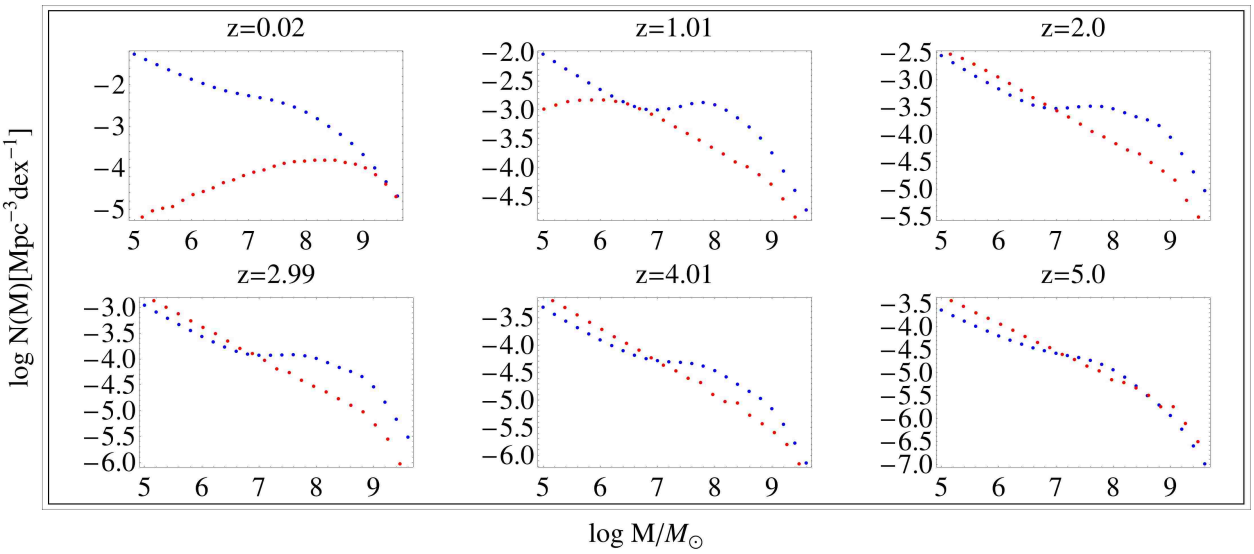

Figure 7.23: Mass function of Model 5b (red) including the effect of mergers on population shown with mass functions from SWM09 in blue. Axes are not scaled the same for each plot.

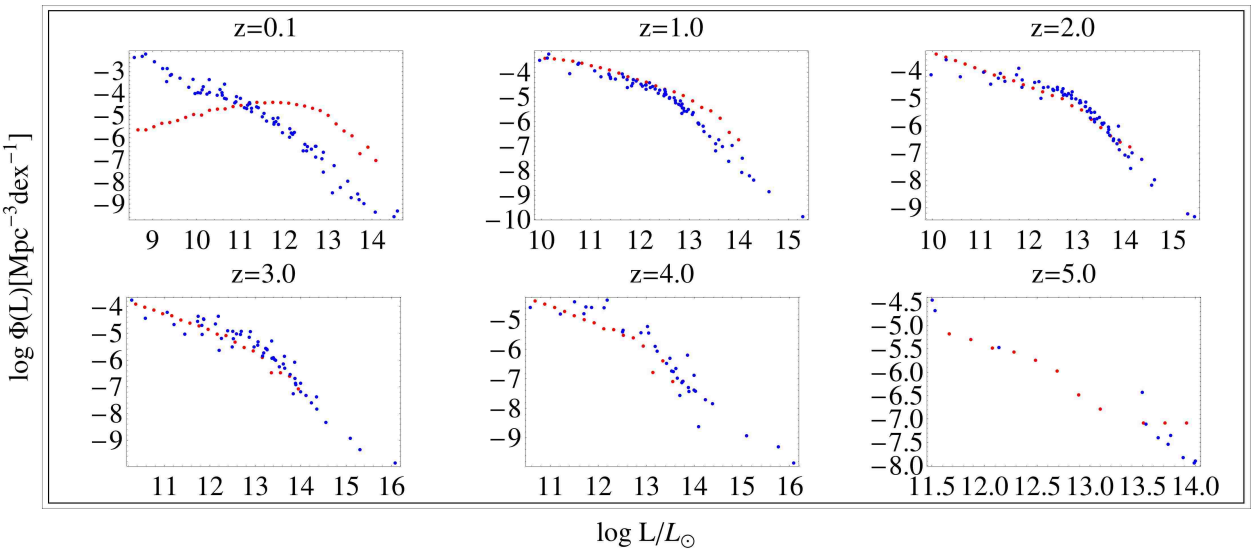

Figure 7.24: Luminosity function of Model 5c (red) including the effect of mergers on population and luminosity. Comparison with HRH07 shown in blue. Axes are not scaled the same for each plot.

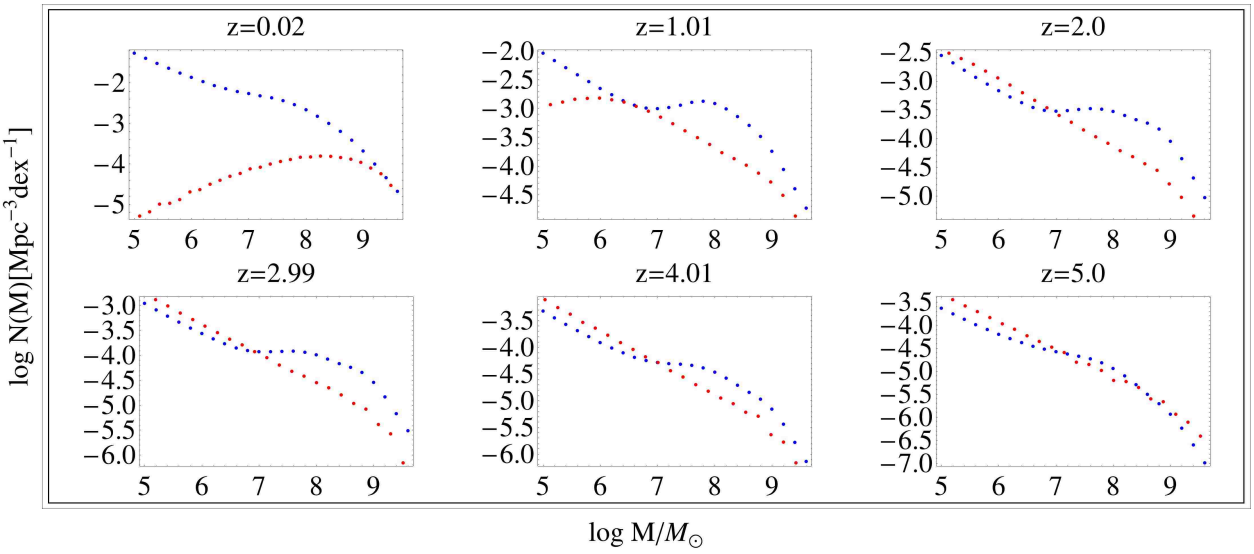

Figure 7.25: Mass function of Model 5c (red) including the effect of mergers on population and luminosity. Comparison with SWM09 shown in blue. This mass function is almost identical to that of Model 5b. There are slight variations at the high mass end due to smaller sample sizes in that regime and the stochastic nature of the accretion and mergers. Axes are not scaled the same for each plot.